2nd International Joint Conference on Water Distribution Systems Analysis & Computing and Control in the Water Industry
Valencia (Spain), 18-22 July 2022
doi: https://doi.org/10.4995/WDSA-CCWI2022.2022.14142

FLOW DYNAMICS IN A PIPE CONTAINING UNEVEN ROUGHNESS ELEMENTS

Katrin Kaur[1], Anatoli Vassiljev[2], Ivar Annus[3], Murel Truu[4] and Nils Kändler[5]

[1,2,3,4,5]Department of Civil Engineering and Architecture, Tallinn University of Technology, Tallinn, Estonia

[1] *katrin.kaur@taltech.ee*, [2] *anatoli.vassiljev@taltech.ee*, [3] *ivar.annus@taltech.ee*, [4] *murel.truu@taltech.ee*, [5] *nils.kandler@taltech.ee*

Abstract

The objective of this study is to improve the methodology for modelling aged pressurised urban networks, such as water distribution system (WDS) pipelines, with substantial and uneven wall roughness. Due to the complexity of the inner surface geometry of old rough pipes, WDS models are unable to predict the real velocities, which are requisite for estimating contamination propagation rates in the system. In order to analyse the impact of inner surface geometry a specifically designed experimental apparatus was built to investigate the flow dynamics in a pipe containing flow-obstructing elements. A transparent pipe was fitted with 3D-printed elements, in two different configurations, at the location of the measurement section and the velocity fields were captured using the particle image velocimetry technique at different flowrates. The experimental results revealed that in the case of one roughness element, the impact to the flow dynamics is local and can be expressed through minor losses, and in the case of multiple elements, the effective diameter of the pipe is reduced and a jet-type flow will develop.

Keywords
Particle image velocimetry, pipe wall build-up, roughness, water distribution system modelling.

1 INTRODUCTION

Degradation of conduits over time results in uneven internal boundaries and concurrently, deviation from design operating conditions. Examination of removed old pipe sections have revealed that the roughness height as well as the shape of the inner pipe surface may vary significantly, resulting in complex geometries. Furthermore, the broadly changing roughness height and distribution will change the pipe effective diameter and flow velocity. Therefore, the determination of real flow velocities in old rough pipes remains a challenge, as even with extensive data collection, it is implausible to determine the pipe roughness values for all links. Among other things, this problem is related to modelling of existing urban water drainage and distribution systems.

Pipes that were originally manufactured with smooth internal surfaces can over time develop irregular wall roughness elements that greatly complicate the flow dynamics [1]. The variation in the geometry of pipe interior due to wall build-up is not only time dependent but is affected by several factors, such as the pipe initial cross-section and material, the water quality, and flow velocity [2]–[5]. Various studies have analysed the growth of the pipe roughness over time, concurrence with flow velocities and quality parameters. [6] reported that the roughness growth depends primarily on the water pH and is linear, with rates ranging from 0.066 to 0.63 mm/yr. The range is in compliance with numerous investigations conducted in the US [7], and results reported by [8]; however, it is significantly lower than the growth rate reported by [9] for galvanized iron pipes (2.13 mm/yr.). The latter are concurrently less often used in WDSs compared to cast iron. A study carried out in Estonia, analysing 25-100 years old metal pipes (steel

and cast iron) with diameters ranging from 75 to 200 mm revealed that the pipe cross-sections were reduced in average by 10% due to wall build-up [2].

Corrosion-induced hydraulic capacity failures due to the pipe wall build-up may prevent WDS from constantly ensuring customer water needs with satisfying quantity and quality [3]. The side effect of corrosion and low velocity can be discolouration of the water, which has been the main customer complaint about the water quality in the UK [4]. The formation and growth of particles in the WDS has diverse driving factors but the sedimentation of the particles is related to the hydraulic conditions of the network. It was shown that at low velocities, the sedimentation will take place in the lower half of the horizontal pipe while at higher velocities, the deposit will cover the entire pipe wall [4]. [5] suggested that the daily peak demands in combination with maximum flow velocity of at least 0.4 m/s can be used to prevent sediment accumulation and concurrent pipe wall build-up.

Data on nominal pipe diameters is generally used in the WDS model initialisation and the pipe wall build-up-induced change in the diameter is compensated by adjusting the pipe roughness [10] or the water consumption at the nodes [11], [12] in the calibration process. Adjusting the consumption is only applicable if it is not measured. Further, in the case of uneven changes in the internal boundary, the practice of adjusting roughness values can lead to estimated unrealistic values larger than pipe radius. Therefore, the latter approach is only suitable for surfaces with easily described geometry [13]. Contrarily, in real WDSs containing old pipes, the inner wall surface will vary significantly, producing complex geometries, and the common practice of using nominal diameters while adjusting the roughness, will result in relatively large errors in flow velocities. Information about real pipe diameters and flow velocities is of utmost importance in estimating the propagation rate of the contaminated zones in WDS in case of chemical or biological threats [14], [15].

Various studies have analysed the flow dynamics in pipes with regular roughness elements, with many of these focusing the main discussion on numerical investigations. [16], [17] investigated the turbulent flow in ribbed pipes and showed that the influence of vortical structures between the ribs on the core flow is dependent on the distance between the ribs. [18], [19] analysed the turbulent flow in corrugated pipes and concluded that the friction factor increases as both the Reynolds number and the groove length increase, and is not affected by the groove height. [20] conducted a study in corrugated pipes, and concluded that contrary to the known formulations of corrugated pipe friction factor, even if the groove width is greater than groove depth, a recirculation zone may occur.

Real old pipe surfaces generally have a range of roughness scales. [1] conducted a series of numerical investigations to model the flow through aged pipes at Reynolds numbers ranging from 6700 to 31 000. They found that the computational fluid dynamics (CFD) models underestimate the friction factors by 8-30% (dependent on Reynolds number and model used). Therefore, improved models, further validated for complex geometries are of high interest. [21] conducted a numerical and experimental investigation on flow in a pipe with an abrupt change in diameter. They concluded that the CFD model with standard k-epsilon turbulence allows to predict the flow dynamics in pipes with complex geometry if moderate changes to the turbulence closure coefficients are made and all geometrical elements that affect the flow are included in the model. [22] investigated the influence of irregular pipe wall roughness numerically and grouped the different types of roughness distributions common to old pipes. [23] investigated the different combinations of roughness elements further and proposed equations for velocity correction for the different wall build-up types based on the numerical study.

The ageing process of pipes should be described in the models not only by the increase of the absolute roughness but also by the reduction of their inner diameter in order to predict the actual flow behaviour more accurately. In addition, in water quality modelling the contamination

propagation and dispersal are strongly coupled with the velocity and turbulence characteristics. Therefore, accurate models capable to simulate the pressurised flow in complex pipelines are crucial for understanding the limits, capacity and need for system's rehabilitation in a more general way. Currently, the modelling approach is also more and more frequently used for different real-time control and management systems and therefore the inaccurate presentation of flow dynamics will potentially hinder the safe operation of the water supply and drainage systems.

Therefore, applying evidence-based assumptions and advanced modelling to define the internal boundaries for the deteriorated pipeline sections is becoming more and more important as we are firstly, entering an era where the average life span of pipes in operation is running out [23] and secondly, more and more real-time control solutions are used to operate WDS. Many of the currently available studies relying on thorough analysis of the modelled velocity field, report validating the models by integral parameters, such as pressure at the in- and outflow of the section of interest. Therefore, more detailed experimental data is needed for the advanced numerical modelling to be practicable.

Herein, the effect of irregular pipe wall build-up to flow dynamics in old rough pipes is investigated experimentally. The aim of the study is to create a comprehensive database of different flow obstruction types and corresponding flow behaviours, and complemented by advanced numerical modelling, map those against different deviations from design operational conditions appearing in real water networks' datasets and give guidelines for the modelling of aged pipelines.

2 EXPERIMENTAL SET-UP

A pipeline apparatus was set up at the Laboratory of Fluid Mechanics, Tallinn University of Technology to investigate the flow dynamics in a pipe containing irregular roughness elements. The experimental investigations were conducted on a transparent pipeline containing different configurations of obstructing roughness elements in the flow domain. The velocity field in the vicinity of the elements was mapped using particle image velocimetry (PIV). The experiments were conducted at different flow rates (Table 1) to characterise the changes of effective flow section in the obstructed conduit.

Table 1. List of experiment. Uncertainty of flow rate measurement reading ±0.5%

Experiment number	Flow rate (Q, l/s)	Reynolds number of the full pipe cross-section (D = 80 mm)
1	3.0	47 900
2	3.8	59 800
3	4.4	69 800
4	5.0	79 300
5	5.6	89 300

The layout of the experimental apparatus is shown on Figure 1. It consists of a tank at the upstream end, a horizontal transparent polymethyl methacrylate pipe with a total length L = 18 m and an internal diameter D = 80 mm, and a PIV measurement section. The upstream tank is fed from, and the pipeline emptied into a 150 cubic meter underground reservoir. The pipeline is

assembled of 2 m long pipes, hydraulically smooth and the outlet is open to atmosphere. Shut-off valves are situated at the up- and downstream end of the pipeline, adjacent to electromagnetic flow meters. The two flow meters are simultaneously used at the experiment initiation stage for the purpose of ensuring that all air is expulsed from the flow domain. The pipeline is pressure driven and the flow rate is controlled by the frequency of the upstream-end pump feeding the tank from the reservoir.

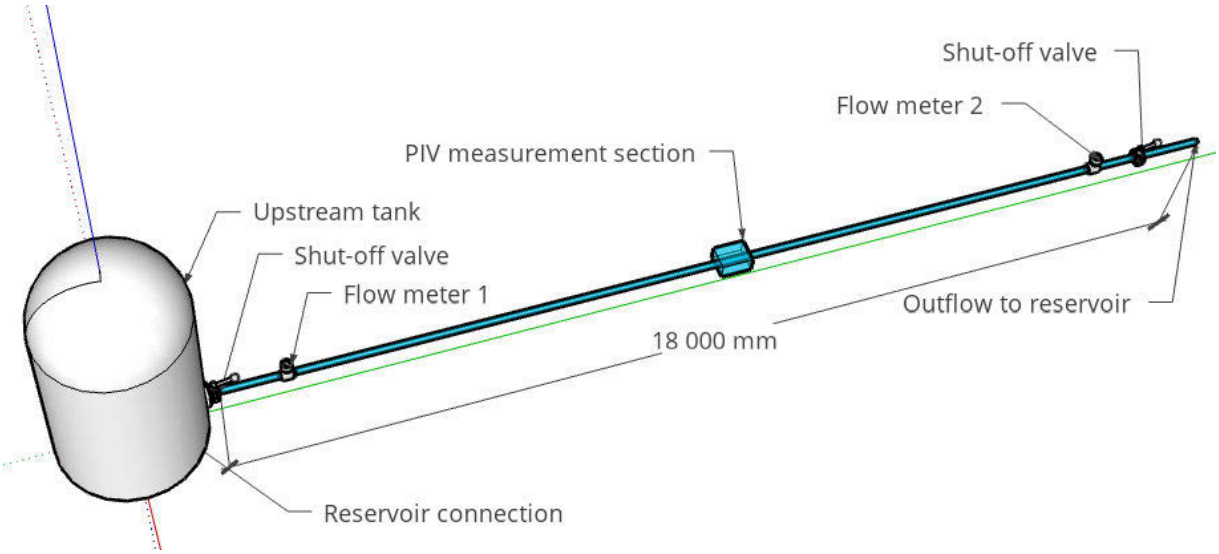

Figure 1. Schematic of the experimental apparatus

A random pattern for an irregular pipe wall build-up element (Figure 2) was created in a numerical study by [22] and obstructing the computational pipe flow domain with different numbers and combinations of these elements was further investigated by [24].

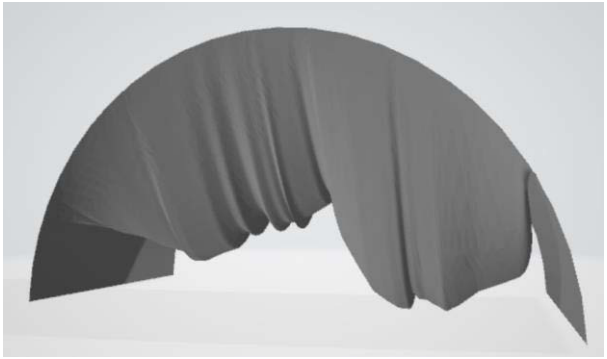

Figure 2. Irregular roughness element used in the experimental study

For this study, a set of the elements were 3D printed and attached inside the pipe of the experimental apparatus. Two configurations of the roughness elements were used for the velocity field measurements at five different flow rates. Firstly, one element was attached to the pipe obvert (Figure 3). Secondly, four elements were inserted into the pipe, two at the obvert and two at the invert, equidistantly (Figure 4).

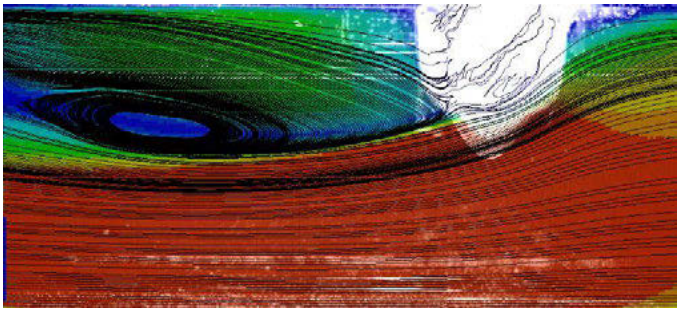

Figure 3. Central plane in the 80 mm pipe with one roughness element located at the pipe obvert. The visual comprises of the image mean, subtracted from the later analyses, streamlines in black, and a scalar map coloured by the axial velocity U. The flow direction is from right to left and a recirculation area occurs behind the element. Red corresponds to highest velocity, blue the lowest.

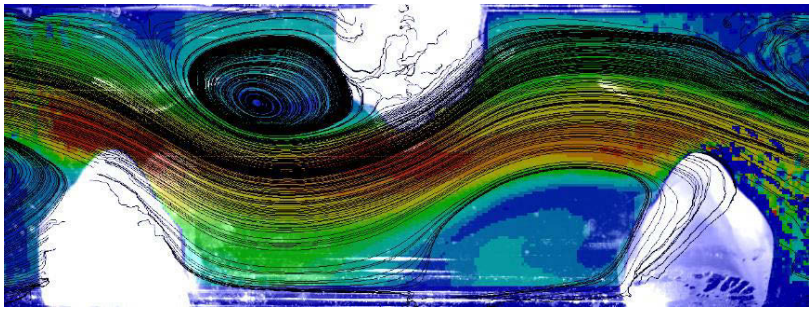

Figure 4. Central plane in the 80 mm pipe with four roughness elements in the investigated area. Three of the elements are in the view range and one is on the right-hand side affecting the inflow into the measurement section. The visual comprises of the image mean, subtracted from the later analyses, streamlines in black, and a scalar map coloured by the axial velocity U. The flow direction is from right to left and recirculation areas occur behind the elements. Red corresponds to highest velocity, blue the lowest.

Changes in the velocity field at the location of interest are measured in the streamwise central plane with two-dimensional PIV. The measurements were carried out using multi-frame single-exposure PIV with a high-speed camera for image capturing, and a continuous-wave laser for creating the light-sheet. The trigger frequency of the camera was adjusted 1000 Hz and the steady state flow was measured for 3 s, which corresponded to 3000 images per experimental run. The data was recorded and processed by Dynamic Studio 4.0 (Dantec Dynamics) software. The cross-correlation method was used to process the PIV data. As a result, velocity vector fields were calculated considering the displacement of the particles between the two frames. An interrogation window of 8 x 8 pixels with 50% overlap was used (1 pix=0.18 mm). The images were pre-processed by subtracting the image mean, getting rid of some minor reflections and the roughness element images in the vector maps. The calibration of the PIV was conducted by capturing a reference images series with rulers inserted into the measurement section. Any distortion in the capturing was avoided by encasing the pipe in a water-filled Plexiglas PIV box and mounting the camera in a horizontal position. Velocities, standard deviations, and variances were calculated using only valid vectors (i.e., gained from measured particle displacements not approximated by the software's algorithm). The average valid vector count for each data point was 1500.

3 RESULTS AND DISCUSSION

The velocity field mapping at different flow rates in the pipe section with one roughness element at the pipe obvert demonstrated how the local disturbance changes the flow dynamics. Namely, how a recirculation area forms and changes in scale with the changing flowrate, indicating a trend in the effective flow area development. The main purpose of these measurements is the creation of a comprehensive dataset for numerical model validation. Figure 5 and Figure 6 present the mapped velocity fields for two experiments.

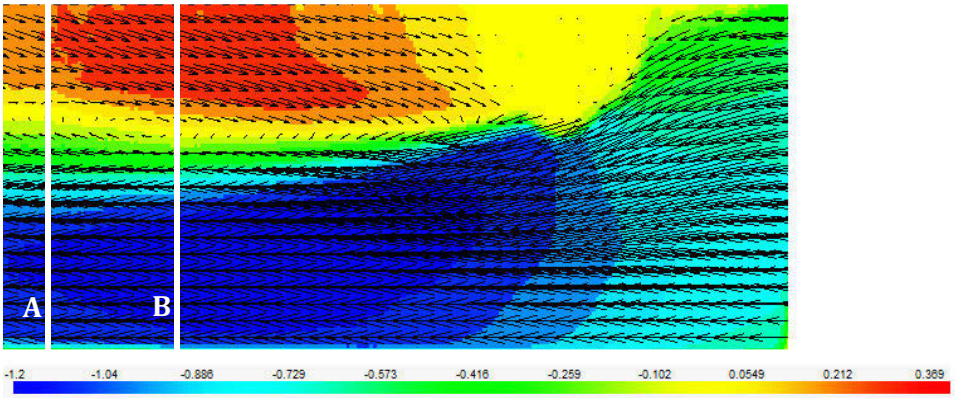

Figure 5. Vector and scalar map. Scalar map coloured by axial velocity U. The scale range -1.2 ... 0.4 m/s. Flow in negative x direction. Flowrate Q=3.0 l/s

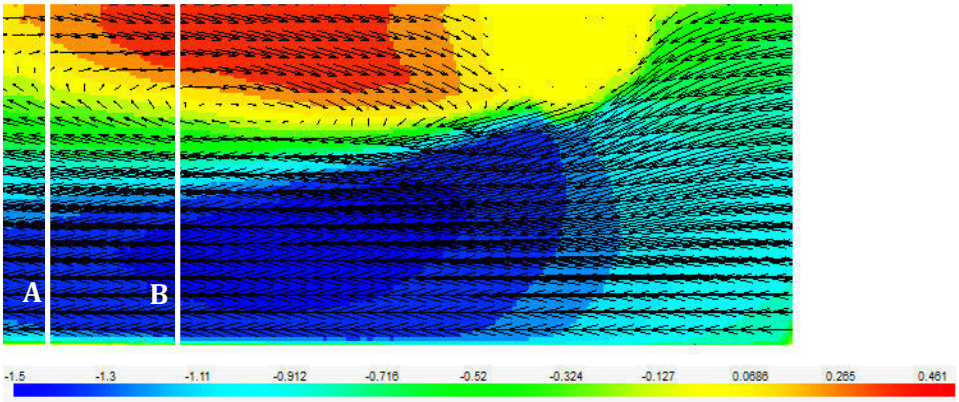

Figure 6. Vector and scalar map. Scalar map coloured by axial velocity U. The scale range -1.5 ... 0.5 m/s. Flow in negative x direction. Flowrate Q=3.8 l/s

Plotting the axial velocity at different sections *A* and *B* (Figure 7 and Figure 8) behind the obstruction reveals that at the nearer location, the higher flowrate yields a larger recirculation area. This agrees in general with the modelling results presented in [22], [24] (Figure 9), where roughness elements of the same type were investigated numerically. It must be noted that the numerical simulations were conducted with more elements in the pipe and at different pipe diameters. Therefore, it can be concluded that the trend is recurring.

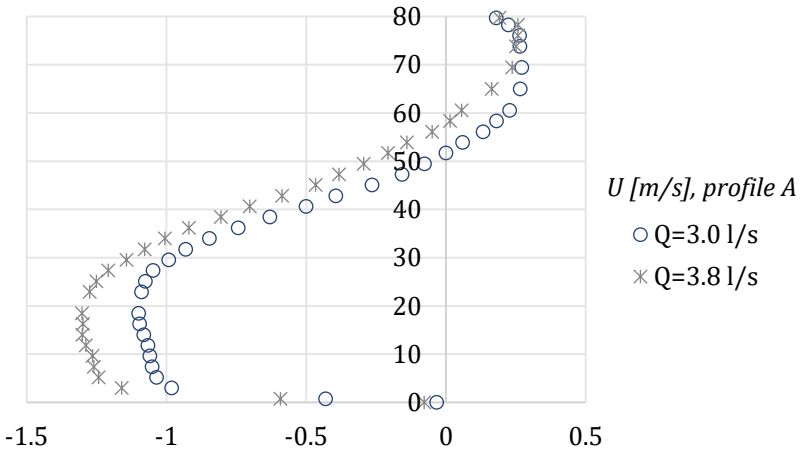

Figure 7. Axial velocity U [m/s] at two flowrates, at location A, in the 80 mm pipe (see Figure 5 and Figure 6)

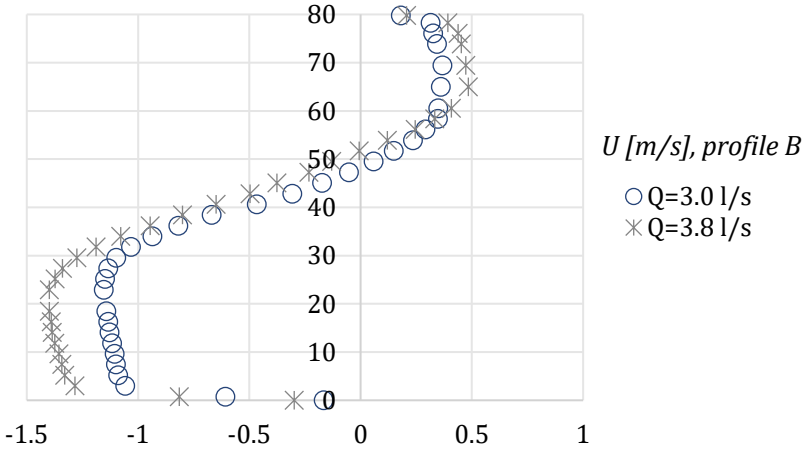

Figure 8. Axial velocity U [m/s] at two flowrates, at location B, in the 80 mm pipe (see Figure 5 and Figure 6)

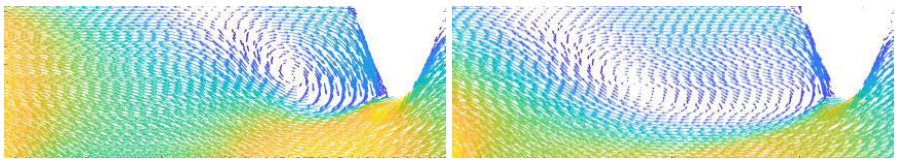

Figure 9. Extract of numerically obtained recirculation area data [22], [24] for qualitative comparison. Lower flowrate on the left hand side and higher on the right.

The velocity field mapping at different flow rates in the pipe section with four elements, two at the obvert and two at the invert, equidistantly, demonstrated clearly the formation of an effective flow area (Figure 10). While under conditions of rising flowrate the recirculation area on the central plane remains roughly the same size, the effective flow section changes. Dynamics at higher flowrates starts to demonstrate that the flow core is diverted from the central plane, forcing higher turbulence generation and forecasting conduit choking.

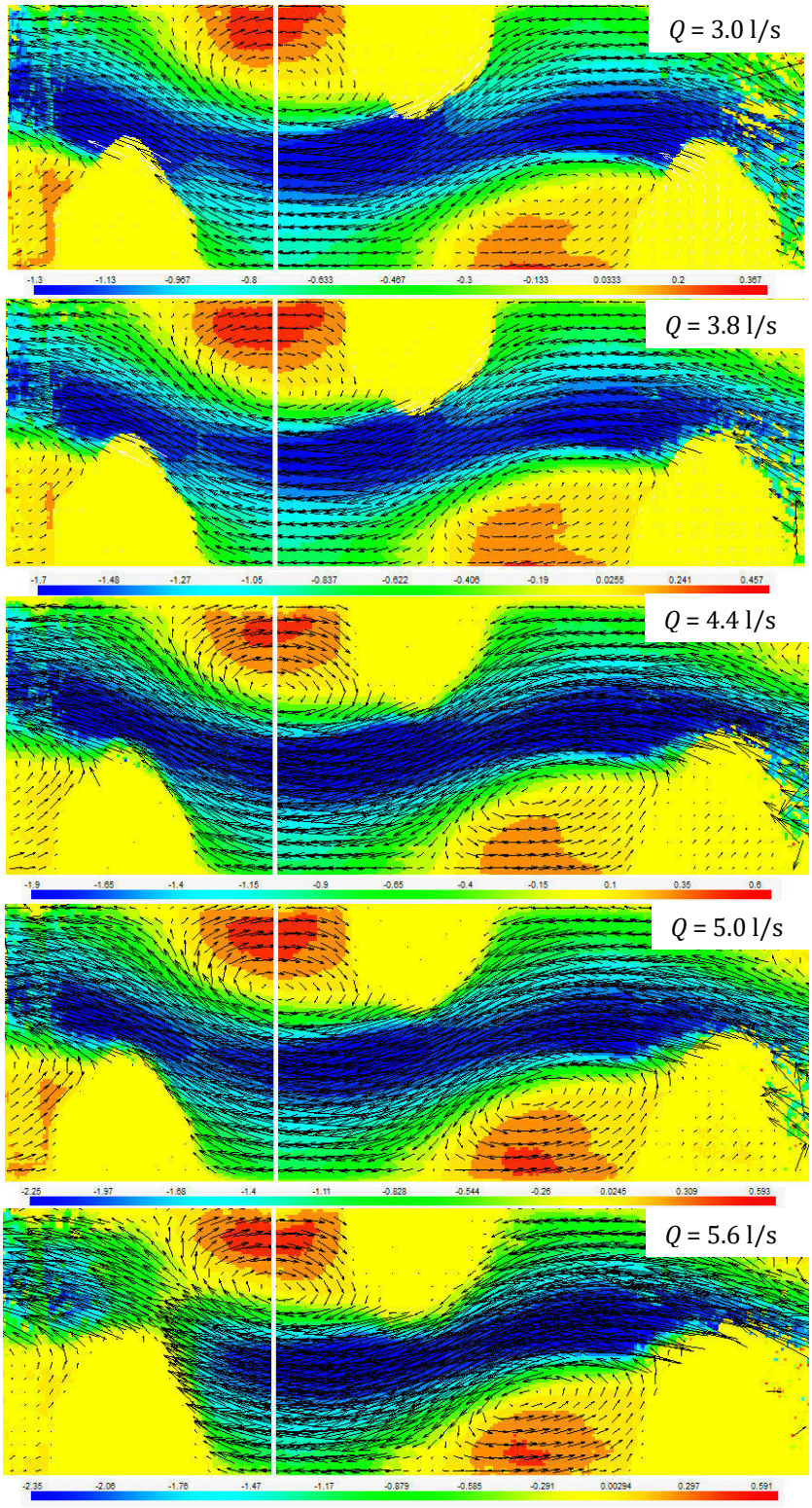

Figure 10. Vector and scalar map in the region of four roughness elements, three of which are in the camera field of view and one on the right hand side, obstructing inflow. Scalar map coloured by axial velocity U. For Q = 3.0 l/s, the scale range is -1.3 … 0.4 m/s; Q = 3.8 l/s, -1.7 … 0.5 m/s; Q = 4.4 l/s, -1.9 … 0.65 m/s; Q = 5.0 l/s, -2.25 … 0.6 m/s; Q = 5.6 l/s, -2.35 … 0.6 m/s. White vertical line – profile location for Figure 11.

Plotting the axial velocity midway between two roughness elements, near the centre of the recirculation area further demonstrates that dead zone (0-velocity) does not shift with the changing of the flowrate (Figure 11). This agrees with the numerical modelling results obtained in [24]. However, it is noteworthy that the modelling failed to indicate the flow choking starting to occur in the experimental measurements.

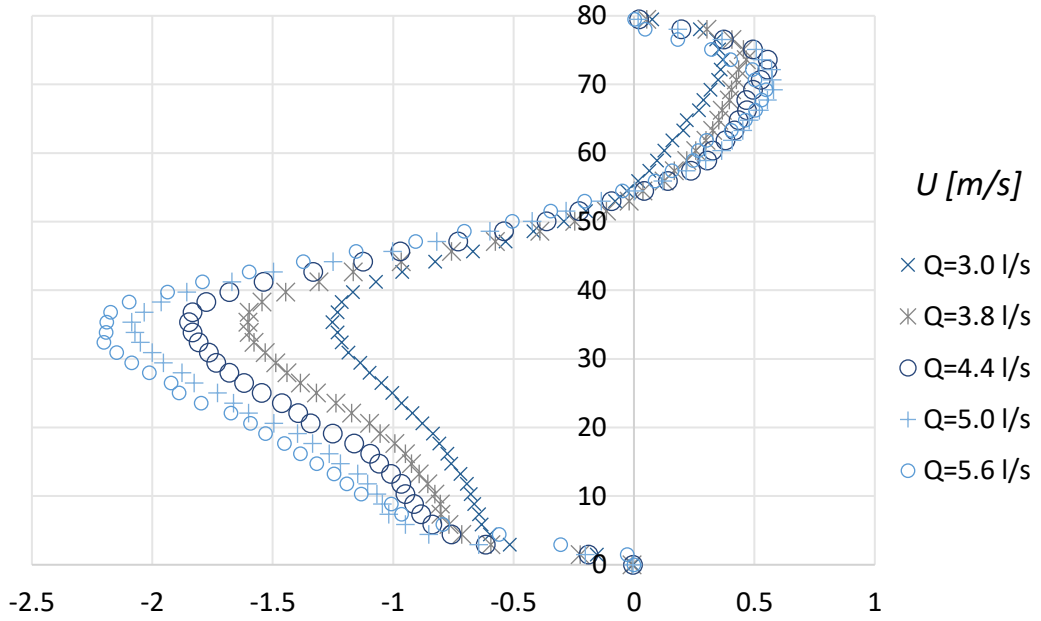

Figure 11. Axial velocity at the location indicated on (Figure 10) for the four roughness elements.

The experimental results reveal that in case of one roughness element the impact to the flow dynamics is local and can be expressed through minor losses. The velocity profiles converge to steady flow profiles downstream of the obstacle as expected. In case of multiple elements, the effective diameter of the pipe is reduced and a jet-type flow will develop at the center of the pipe. Therefore, the actual flow velocity can be times higher compared to the velocity in new pipes with nominal diameter. The changes in velocity increase the pressure drop in the system leading to unrealistic estimations of pipe roughness used in the hydraulic models of WDS.

4 CONCLUSIONS

Understating the flow dynamics in deteriorated pipeline sections is more relevant than ever as we are entering an era where the average life span of pipes in operation is running out, and concurrently, applying real-time control solutions is becoming more commonplace. While many authors recommend making use of advanced numerical modelling (viz. CFD), there are scarce experimental studies that would provide comprehensive calibration and validation opportunities for these complex models, where grid and time resolution, choice of turbulence models and correct treatment of boundaries, among other things, have the capacity to change the output not only qualitatively, but also quantitively.

Herein, the effect of irregular pipe wall build-up to flow dynamics in old rough pipes is investigated experimentally. The aim of the study is to create a comprehensive database of different flow obstruction types and corresponding flow behaviours. PIV was used to map the velocity fields in the pipe containing obstacles.

It was found that the experimental results preliminarily further support the previously published numerical studies of the authors. However, the experiments revealed some dynamics not

witnessed in the computational results. The PIV measurements were conducted for two geometric configurations for five different flowrates. Plotting the axial velocity at different sections behind the one obstruction revealed that at the nearer location, the higher flowrate yields a larger recirculation area when comparing flowrates Q = 3.0 l/s and Q = 3.8 l/s. However, investigating the remaining flowrates of this experimental series revealed diverging results as compared to modelling and merit further investigation. Analysing the velocity field in the pipe with four roughness elements revealed that at higher flowrates the flow core is diverted from the central plane, forcing higher turbulence generation and forecasting conduit choking.

To create an extensive validation database and to develop a comprehensive methodology for determining the proper ratio of roughness and effective diameter in the WDS models based on pipe material and age, further experimental investigations are needed. The authors plan to conduct further experiments on the herein presented configurations of roughness elements and to test new configurations, too.

5 ACKNOWLEDGEMENTS

The research was supported by the Estonian Research Council grant PRG667.

6 REFERENCES

[1] R. T. Christensen, R. E. Spall, and S. L. Barfuss, “Application of Three RANS Turbulence Models to Aged Water Transmission Pipes,” Journal of Hydraulic Engineering, vol. 137, no. 1, pp. 135–139, 2011.

[2] N. Kändler, “Optimal algorithm for rehabilitation of a water distribution network,” Tallinn University of Technology, Tallinn, Estonia, 2002.

[3] V. K. Kanakoudis, “A troubleshooting manual for handling operational problems in water pipe networks,” Journal of Water Supply: Research and Technology-Aqua, vol. 53, no. 2, pp. 109–124, 2004.

[4] I. J. H. G. Vreeburg and Dr. J. B. Boxall, “Discolouration in potable water distribution systems: A review,” Water Research, vol. 41, no. 3, pp. 519–529, 2007.

[5] J. H. G. Vreeburg, E. J. M. Blokker, P. Horst, and J. C. van Dijk, “Velocity-based self-cleaning residential drinking water distribution systems,” Water Supply, vol. 9, no. 6, pp. 635–641, 2009.

[6] C. F. Colebrook and C. M. White, “Experiments with fluid friction in roughened pipes,” Proceedings of the Royal Society of London. Series A: Mathematical and Physical Sciences, vol. 161, no. 906, pp. 367–381, 1937.

[7] W. W. Sharp and T. M. Walski, “Predicting Internal Roughness in Water Mains,” Journal American Water Works Association, vol. 80, no. 11, pp. 34–40, 1988.

[8] G. S. Williams and A. Hazen, Hydraulic Tables. Chapman & Hall, 1920.

[9] G. Echávez, “Increase in Losses Coefficient with Age for Small Diameter Pipes,” Journal of Hydraulic Engineering, vol. 123, no. 2, pp. 157–159, 1997.

[10] K. E. Lansey, W. El-Shorbagy, I. Ahmed, J. Araujo, and C. T. Haan, “Calibration Assessment and Data Collection for Water Distribution Networks,” Journal of Hydraulic Engineering, vol. 127, no. 4, pp. 270–279, 2001.

[11] V. Kanakoudis and K. Gonelas, “Accurate water demand spatial allocation for water networks modelling using a new approach,” Urban Water Journal, vol. 12, no. 5, pp. 362–379, 2015.

[12] V. Kanakoudis and K. Gonelas, “Properly allocating the urban water meter readings to the nodes of a water pipe network simulation model,” Desalination and Water Treatment, vol. 54, no. 8, pp. 2190–2203, 2015.

[13] J. Jiménez, “Turbulent flows over rough walls,” Annual Review of Fluid Mechanics, vol. 36, no. 1, pp. 173–196, 2004.

[14] J. B. Boxall, A. J. Saul, and P. J. Skipworth, “Modeling for Hydraulic Capacity,” Journal - American Water Works Association, vol. 96, no. 4, pp. 161–169, 2004.

[15] I. Annus and A. Vassiljev, “Different Approaches for Calibration of an Operational Water Distribution System Containing Old Pipes,” Procedia Engineering, vol. 119, pp. 526–534, 2015.

[16] S. Vijiapurapu and J. Cui, “Simulation of Turbulent Flow in a Ribbed Pipe Using Large Eddy Simulation,” Numerical Heat Transfer, Part A: Applications, vol. 51, no. 12, pp. 1137–1165, 2007.

[17] S. Vijiapurapu and J. Cui, “Performance of turbulence models for flows through rough pipes,” Applied Mathematical Modelling, vol. 34, no. 6, pp. 1458–1466, 2010.

[18] H. Stel, R. E. M. Morales, A. T. Franco, S. L. M. Junqueira, R. H. Erthal, and M. A. L. Gonçalves, “Numerical and Experimental Analysis of Turbulent Flow in Corrugated Pipes,” Journal of Fluids Engineering, vol. 132, no. 7, p. 071203, 2010.

[19] H. Stel, A. T. Franco, S. L. M. Junqueira, R. H. Erthal, R. Mendes, M. A. L. Gonçalves, and R. E. M. Morales, “Turbulent Flow in D-Type Corrugated Pipes: Flow Pattern and Friction Factor,” Journal of Fluids Engineering, vol. 134, no. 12, 2012.

[20] F. Calomino, A. Tafarojnoruz, M. De Marchis, R. Gaudio, and E. Napoli, “Experimental and Numerical Study on the Flow Field and Friction Factor in a Pressurized Corrugated Pipe,” Journal of Hydraulic Engineering, vol. 141, no. 11, 2015.

[21] I. Annus, A. Kartushinsky, A. Vassiljev, and K. Kaur, “Numerical and Experimental Investigation on Flow Dynamics in a Pipe With an Abrupt Change in Diameter,” Journal of Fluids Engineering, vol. 141, no. 10, p. 101301, 2019.

[22] I. Annus, A. Vassiljev, N. Kändler, and K. Kaur, “Determination of the corresponding roughness height in a WDS model containing old rough pipes,” Journal of Water Supply: Research and Technology-Aqua, vol. 69, no. 3, pp. 201–209, 2020.

[23] AWWA, “Dawn of the Replacement Era: Reinvesting in Drinking Water Infrastructure,” United States of America Water Works Association, Denver, USA, 2001.

[24] K. Kaur, A. Vassiljev, I. Annus, N. Kändler, and J. Roosimägi, “Numerical investigation of the impact of irregular pipe wall build-up on velocity in the water distribution system,” Journal of Water Supply: Research and Technology-Aqua, vol. 69, no. 7, pp. 647–655, 2020.